

# Evaluation of magnitude- and phase-correct unit-force transfer functions for the structural description of electrical machines

Michael Schröder\*, David Franck and Kay Hameyer  
*Institute of Electrical Machines, RWTH Aachen University, Aachen, Germany*

**Abstract.** The structural dynamic simulation of electrical machines is an appropriate tool to improve electrical machines in an early design stage, in consideration of their acoustic and vibration properties. In order to reduce the calculation effort, a time efficient method is desirable. Unit-force transfer functions describe the linear behavior of the structure when it is excited with unit-force waves in the machine's air gap. In this paper, magnitude- and phase-correct transfer functions are simulated numerically for an exemplary machine and then verified by measurements. With those transfer functions, the structural response of the machine can be calculated fast for different operating points.

Keywords: Structural dynamic simulation, structural description, electrical machine, acoustic, vibration, unit-force, complex transfer function

## 1. Introduction

The magnetic flux density in the air gap of a permanent magnet synchronous machine (PMSM) is caused by the windings supplied with current in the stator on the one hand and the permanent magnets in the rotor on the other hand. Both field parts result in the magnetic air gap field, where electrical energy is transformed in mechanical energy and vice versa. Because of harmonics, the magnetic flux density in the air gap can be described by the FOURIER series expansion

$$\vec{B}(\varphi, t) = \sum_{\nu=0}^{\infty} \vec{B}_{\nu} \cdot \cos(\nu \cdot \varphi - \omega_{\nu} \cdot t - \phi_{\nu}), \quad (1)$$

where  $\vec{B}_{\nu}$  is the amplitude of the flux density of mode  $\nu$  with angular frequency  $\omega_{\nu}$  and phase angle  $\phi_{\nu}$  [1].  $\varphi$  is the coordinate in circumferential direction in cylinder coordinates. The force density at the intersection between the machine's air gap and the stator can be derived from the LORENTZ force and simplified by means of the MAXWELL stress tensor [2]. This results in the well-known equations for the tangential component of the force density

$$\sigma_{\text{tan}}(\varphi, t) = \frac{1}{\mu_0} \cdot B_{\text{rad}}(\varphi, t) \cdot B_{\text{tan}}(\varphi, t) \quad (2)$$

---

\*Corresponding author: Michael Schröder, Institute of Electrical Machines, RWTH Aachen University, Schinkelstraße 4, D-52056 Aachen, Germany. Tel.: +49 241 80 97667; Fax: +49 241 80 92270; E-mail: michael.schroeder@iem.rwth-aachen.de.

and the radial component

$$\sigma_{\text{rad}}(\varphi, t) = \frac{1}{2\mu_0} \cdot (B_{\text{rad}}^2(\varphi, t) - B_{\text{tan}}^2(\varphi, t)) \approx \frac{1}{2\mu_0} \cdot B_{\text{rad}}^2(\varphi, t). \quad (3)$$

The magnetic permeability  $\mu$  of the ferromagnetic material is much higher than in the air gap (e.g.  $\mu_{\text{Fe}} \approx 10\,000 \gg \mu_{\text{Air}} \approx 1$ ). For this reason the magnetic flux lines run predominantly in radial direction through the air gap, so that the radial flux density  $B_{\text{rad}}(\varphi, t)$  is much higher than the tangential one  $B_{\text{tan}}(\varphi, t)$ . This results in the simplified approximation in Eq. (3) [3,4]. The tangential force density  $\sigma_{\text{tan}}(\varphi, t)$  is necessary for the torque production in the electrical machine. The integral over the tangential force density along the air gap in circumferential direction yields the torque  $M$ . The radial force density otherwise acts on the stator teeth. It deforms the stator yoke in radial direction and is so essentially the reason for sound radiation. Radial force density deforms the stator yoke also tangential, but comparatively low and so negligible for sound radiation. Similarly tangential force components cause tangential and radial deformation of the stator yoke, but also small in comparison to the radial force components. So it is adequate to limit on the radial force density [5]. As shown in Eq. (1), the magnetic flux density can be described by a FOURIER series expansion. The magnetic forces can be described equally. The forces deform the stator just in a range of micrometers, which does not end in ductile deformation. Therefore, the electrical machine can be determined as a linear and time-invariant system and the effect of each magnetic force wave

$$\vec{F}_\nu = \vec{F}_\nu \cdot \cos(\nu \cdot \varphi - \omega_\nu \cdot t - \phi_\nu) \quad (4)$$

can be investigated separately [1,5]. So the magnetic force distribution in the air gap of an electrical machine caused by the magnetic field can be described as a sum of rotating force waves. The definition of unit-waves is introduced in [6,7]. Unit-waves are force waves with amplitude of 1 N and a specific mode order  $\nu$ . The quantity, which describes the structure's dependency from different unit-waves, is called unit-wave response or unit-force response, as depicted in [4,8]. The difference between the classical frequency response and the unit-force response is the type of excitation. Whereas the structure is excited at discrete points in order to obtain the frequency response, it is excited with a rotating force wave distribution to get the unit-force transfer functions [7].

## 2. Machine model

The electrical machine under study is a PMSM with  $N_1 = 6$  stator teeth, single tooth windings and  $p = 2$  pole pairs. To simulate the machine in an acceptable time frame, the following simplifications are done to the machine's structural dynamic model. Attached parts, such as the encoder, are removed from the model. The coils are removed as well and are replaced by additional masses added to the stator teeth. Bolted assemblies are eliminated, the boreholes are closed and substituted by contact elements. The bearings are modeled by means of a cylinder with adjusted material properties. This results in a discretized machine model with 149 978 solid elements, 25 367 contact elements and 260 089 nodes as shown in Fig. 1. The boundary condition at the bottom of the machine's mounting plate is set to fixed support. For the laminated stator and rotor, transversal isotropic material properties are used. Transversal isotropy is a special case of orthotropy, where the material is isotropic in one plane and anisotropic in one direction. Therefore, this case of material characterization is convenient for the description of electrical machines, whose rotor and stator consist of multiple layers of core laminations in axial direction. For this case, HOOKE's matrix can be built up of five independent matrix elements.

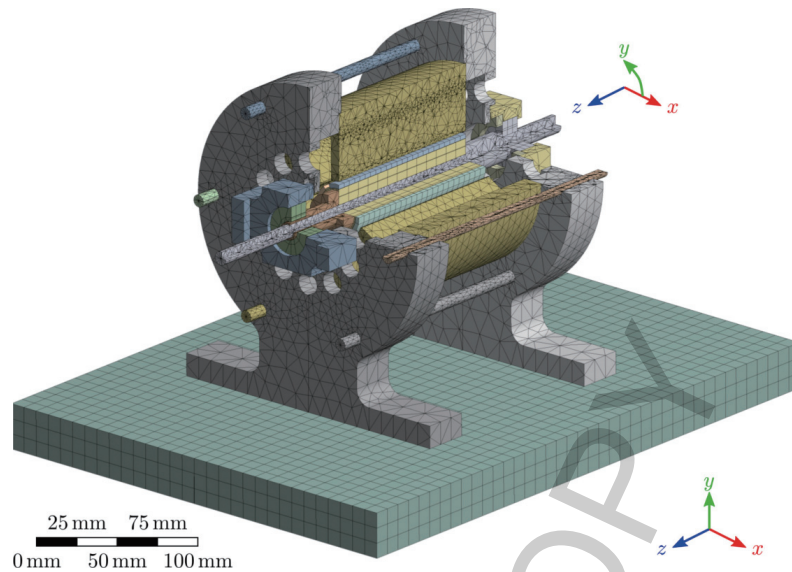


Fig. 1. Meshed machine's structural dynamic model, with 149 978 solid elements, 25 367 contact elements and 260 089 nodes. Shown are a sectional representation and the used coordinate systems.

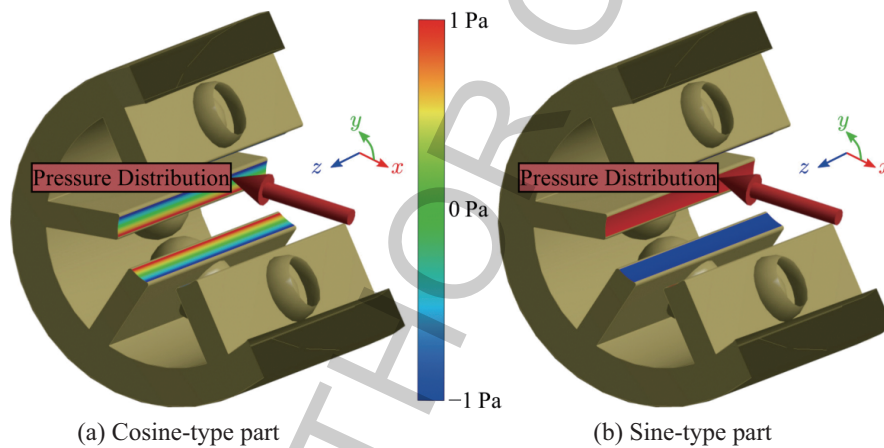


Fig. 2. Radial unit-force pressure distribution exemplary for the exciting force mode 3 with magnitude of  $1 \text{ N/m}^2$  is imposed directly to the stator teeth. (a) Cosine-type part. (b) Sine-type part.

### 3. Numerical determination of the unit-force transfer functions

The determination of the unit-force transfer functions is done with a harmonic response analysis, because the forces in an electrical machine occur cyclic per revolution. Radial unit-force density waves with magnitude of  $1 \text{ N/m}^2$  are imposed directly to the stator teeth. The radial force density waves have to be defined in a rotating way in the analysis. This is done with a cosine-type pressure distribution along the stator teeth and a spatial superimposed sine-type pressure distribution, with same amplitude, phase shifted by  $\pi/2$ . The equation for the radial force density of mode  $\nu$  at stator position  $\varphi$  and point in time  $t$

is than in common notation

$$\sigma_{\text{rad},\nu}(\varphi, t) = \text{Re} \left\{ \hat{\sigma}_{\nu}(\omega) \cdot \left( \cos(\nu\varphi) + j \sin(\nu\varphi) \right) \cdot e^{-j(\omega t + \phi)} \right\}. \quad (5)$$

Figure 2 shows the cosine-type part and the sine-type part of the radial unit-force pressure distribution exemplary for the exciting force mode 3. The simulation has to be conducted for all relevant force modes. The cases  $\nu = 0$ ,  $\nu = 1$  and  $\nu = 2$  are important. The breathing mode ( $\nu = 0$ ) is a pure tensile load for the stator. It is studied in detail in [9]. The case  $\nu = 1$ , the so called beam bending mode can be interpreted as a vibration force, acting on the rotor's balance point [5]. For the ovaling mode  $\nu = 2$  and higher modes finally, just the stator is deformed. With increasing mode order, the influence of the excitation decrease, so that for this simulation the mode orders 0 to 5 are examined. During the simulation, the solver iterates over angular velocities  $\omega$  from 500 Hz up to 4000 Hz and calculates the complex displacement in  $x$ -,  $y$ - and  $z$ -direction of every node on the machine's surface (1596 nodes for the machine under study). The area between 0 and 500 Hz is not calculated, because there are no machine's eigenfrequencies, as a modal analysis of the machine has shown. The modal analysis was conducted as described in [10,11]. To calculate the unit-force transfer functions for the radial surface displacement, velocity and acceleration, the complex velocity and complex acceleration are calculated from the complex displacement in frequency domain by

$$\underline{a}(\omega) = j\omega \cdot \underline{v}(\omega) = -\omega^2 \cdot \underline{\xi}(\omega). \quad (6)$$

This operation is carried out for all the node's components and for every extracted frequency. Afterward the  $x$ -,  $y$ - and  $z$ -components of displacement, velocity and acceleration are transformed in a radial and a tangential component. To assess the force mode's influence on the expansion modes, a circular ring in the middle of the machine surface is examined. A spatial discrete FOURIER transformation (DFT) across all points on the ring is performed for every frequency. So it can be ascertained, which expanding mode orders dominate in the modal superposition.

Figure 3 shows the magnitude of the simulated unit-force transfer functions for surface velocity with reference to pressure over frequency. For the studied machine, the first six exciting force modes 0 to 5 and the first six expanding modes 0 to 5 are shown. A comparison of the six diagrams in Fig. 3 shows, that expanding mode 1 is rarely excited. As well as the other uneven expanding modes of order 3 and 5, which are excited comparatively low. Dominant are the even expanding modes with order 0 and 2 as well as order 4. The resonance frequencies, which can be identified in the unit-force transfer functions, coincide with the eigenfrequencies, calculated in a modal analysis.

#### 4. Experimental verification of the transfer functions

During a slow machine's run-up, the surface acceleration at a point in the middle of the stator is measured. In addition, the rotor angle and the currents of two stator phases are recorded. During the slow run-up, single machine's resonance frequencies are passed through. Because it is not possible to excite those frequencies in an infinitesimal period, the run-up speed is limited in order to pass as much energy as possible into the structure [2]. The force density cannot be determined by measurement techniques. On this account, the force density is calculated out of the current propagation over one mechanical revolution of the rotor via finite element simulation, as described in [6]. The simulation

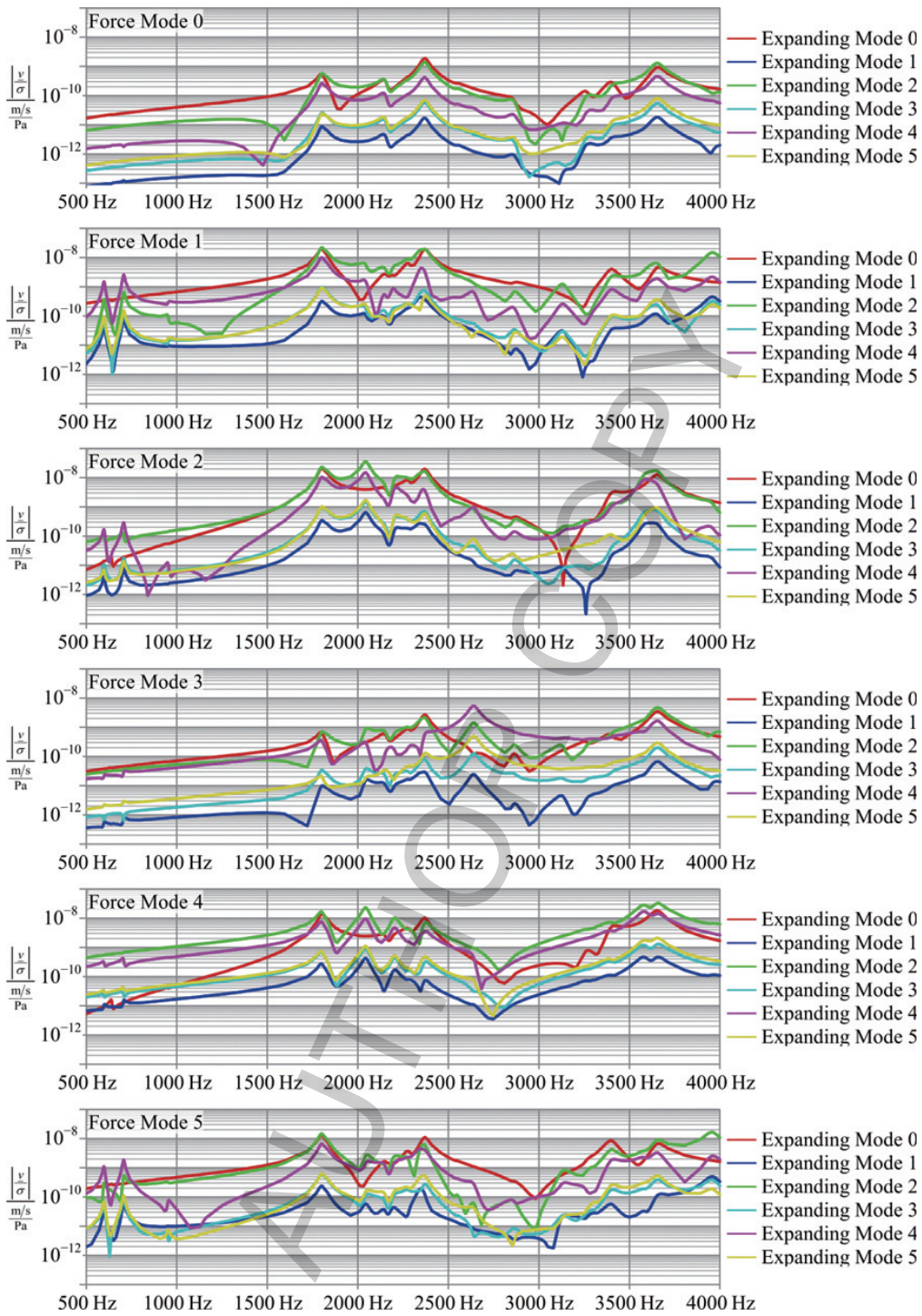


Fig. 3. Magnitude of the simulated unit-force transfer functions for surface velocity with reference to pressure over frequency. Shown are the first six expanding modes for the first six exciting force modes.

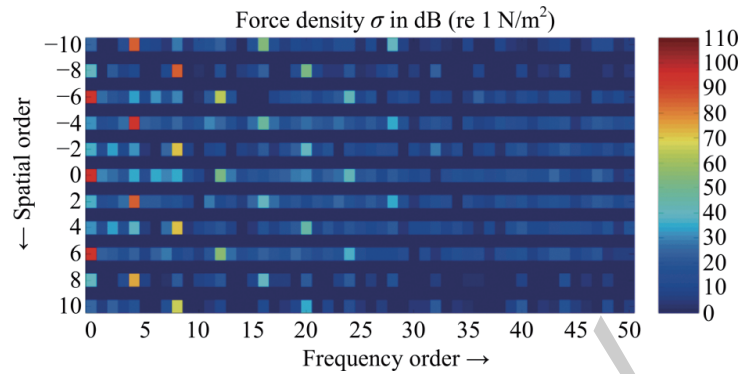


Fig. 4. Magnitude of the calculated force density  $\sigma$  in dB (re 1 N/m<sup>2</sup>) for spatial orders  $-10$  to  $10$  and frequency orders from  $0$  up to  $50$ . Basis for the calculation are the measured machine currents for one mechanical revolution of the rotor.

yields force densities as a function of time and space. A 2-D-DFT transforms the force densities to space and frequency domain and produces the force density matrix  $\sigma$ , containing the required magnitudes of the force density waves as shown in Fig. 4. The force density's magnitude decreases with increasing frequency order. This behavior is comparable to [10]. The magnitude of every fourth frequency order is distinctive. This is because of the machine's pole pair number of  $p = 2$ , which is conform to four poles. The same behavior can be seen for the spatial order, where every sixth order dominates. This matches with the number of stator teeth.

The surface velocity  $v$  is calculated during the measurements out of the surface acceleration by integration. To determine the transfer functions, the surface velocity is multiplied with the inverse  $\sigma^{-1}$  of the force density matrix [12]:

$$\vec{v}(\omega) = \sigma \cdot \vec{H}(\omega) \Rightarrow \vec{H}(\omega) = \sigma^{-1} \cdot \vec{v}(\omega). \quad (7)$$

The force density matrix  $\sigma$  is not compulsory quadratic and nonsingular. For this reason, the MOORE-PENROSE pseudoinverse  $\sigma^+$  is calculated, which exists even for singular and nonquadratic matrices. For calculation of the pseudoinverse, the density matrix must have full column rank. Furthermore, arbitrary orders can be used, which leads to an overdetermined system of equations. This is solved by the method of least squares. In order to check the calculated transfer functions, they are multiplied with the force density matrix. In the case the system of equations is overdetermined it is possible that there are multiple solutions of the pseudoinverse. For this reason, a correction factor is determined out of the calculated and the measured velocity matrix, which is then multiplied with the transfer functions matrix. The so evaluated transfer functions show that the force mode of the fourth order excited the machine the most. As well as the other even force modes of order  $0$  and  $2$ , which lead to an excitation of the machine. The transfer functions for the uneven force modes  $1$ ,  $3$  and  $5$  are lesser in size, because they are not excited by the force density waves (compare Fig. 4). A comparison with the numerical determined unit-force transfer functions (see Fig. 3) shows that the transfer functions excited by even force modes are in the same dimension. The transfer functions excited by uneven force modes are much smaller than the simulated ones. An adaption of the material parameters YOUNG's modulus, POISSON's ratio and shear modulus [11] used in the numerical simulation is recommended. Thus, the simulation quality can be improved and the deviance between measurement and calculation can be minimized as described in [4].

## 5. Conclusion

An approach for the evaluation of magnitude- and phase-correct unit-force transfer functions for structural dynamic simulations is presented. Complex transfer functions are calculated for an exemplary machine. This is done with a harmonic analysis. For this purpose, rotating radial unit-force density waves are imposed directly to the stator teeth. The transfer functions are determined for surface velocity with reference to pressure on a circular ring in the middle of the machine's surface. The evaluated transfer functions are verified by test bench measurements. A force density distribution must be calculated out of the rotor angle and the phase currents, because it cannot be determined by measurement techniques. The surface acceleration is measured at a point in the middle of the stator. For calculating the transfer functions, the MOORE-PENROSE pseudoinverse is necessary. The comparison shows that the measured transfer functions are in the same dimension as the calculated for the even force modes. The determining and adaption of material properties for the simulation is essential. With the evaluated transfer functions, the machine's surface velocity can be calculated fast for different types of force density excitations at different machine's operating points. The transfer functions deliver more detailed prediction concerning sound radiation than simple cylinder models (compare [5]). They are relevant for full transient machine models (introduced in [12]) or multi-physics lumped models as presented in [10,11].

## References

- [1] H.O. Seinsch, *Oberfelderscheinungen in Drehfeldmaschinen – Grundlagen zur analytischen und numerischen Berechnung*, Stuttgart: Teubner, 1992.
- [2] D.J. Griffiths, *Introduction to Electrodynamics*, (3rd Edition), New Jersey: Prentice Hall, 1999.
- [3] J.F. Gieras, C. Wang and J. Cho Lai, *Noise of polyphase electric motors*, USA: CRC Press (Taylor & Francis Group), 2006.
- [4] M.v.d. Giet, *Analysis of electromagnetic acoustic noise excitations: A contribution to low-noise design and to the auralization of electrical machines*, *Dissertation, Aachen: Shaker Verlag* (2011).
- [5] H. Jordan, *Geräuscharme elektromotoren – lärm-bildung und lärm-beseitigung bei elektromotoren*, Essen: Verlag W. Girardet, 1950.
- [6] J. Roivainen and A. Makinen, Unit-wave response-based computation of magnetic noise of electric machines, *IEEE International Conference on Industrial Technology (ICIT)* (2010), 439–444.
- [7] J. Roivainen, Unit-wave response-based modeling of electromechanical noise and vibration of electrical machines, *Dissertation, Helsinki: University of Technology* (2009).
- [8] M.v.d. Giet, J. Blum, P. Dietrich, S. Pelzer, M. Müller-Trapet, M. Pollow, M. Vorländer and K. Hameyer, Auralization of electrical machines in variable operating conditions, *IEEE International Electric Machines & Drives Conference (IEMDC)*, (2011), 1462–1467.
- [9] T.E. McDevitt, R.L. Campbell and D.M. Jenkins, An investigation of induction motor zeroth-order magnetic stresses, vibration, and sound radiation, *IEEE Transactions on Magnetics* **40**(2) (2004), 774–777.
- [10] N. Bracikowski, M. Rossi, M. Hecquet and F. Gillon, Multi-physics design rules using lumped models for a permanent magnet synchronous machine, *International Journal of Applied Electromagnetics and Mechanics* **43**(1–2) (2013), 13–23.
- [11] N. Bracikowski, *Modélisation multi-physique par modèles à constantes localisées; Application à une machine synchrone à aimants permanents en vue de son dimensionnement*, *Dissertation, PRES Université Lille Nord-de-France*, (2012).
- [12] D. Franck, T. Herold and K. Hameyer, *Transient acoustic simulations of electrical drive-trains*, *DAGA*, (2013).